Accurate Measurements of the Acoustical Physical Constants of Synthetic α-Quartz for SAW Devices

Jun-ichi Kushibiki, *Member, IEEE*, Izumi Takanaga, *Member, IEEE*, and Shouichi Nishiyama

***Abstract*—Accurate measurements of the acoustical physical constants (elastic constants, piezoelectric constants, dielectric constants, and density) of commercially available and widely used surface acoustic wave (SAW)-grade synthetic α-quartz are reported. The propagation directions and modes of bulk waves optimal for accurately determining the constants were selected through numerical calculations, and three principal X-, Y-, and Z-cut specimens and several rotated Y-cut specimens were prepared from a single crystal ingot to determine the constants and to confirm their accuracy. All of the constants were determined through highly accurate measurements of the longitudinal velocities, shear velocities, dielectric constants, and density. The velocity values measured for the specimens that were not used to determine the constants agreed well with those calculated from the determined constants, within a difference of ± 0.20 m/s ($\pm 0.004\%$).**

I. Introduction

ALPHA-QUARTZ has been widely used as substrate material for bulk acoustic wave devices and SAW devices because of its vibration modes with zero temperature coefficients at room temperatures and its remarkable physical and chemical stability. It is essential to have detailed and precise knowledge of the acoustical physical constants (elastic constant c^E, piezoelectric constant e, dielectric constant ε^S, and density ρ) for designing devices and for calculating the propagation characteristics of bulk waves and SAWs. As quartz is an important material for time and frequency standards, the constants have been extensively studied and reported by Mason [1], Bechmann *et al.* [2], Koga *et al.* [3], and many other investigators. However, there has been a lack of information and detail in some of the previous reports. Some of the reports did not provide the sources and growth conditions of the crystals used, and some presented the constants determined using specimens cut from several crystals grown under different conditions, even though it is known that the acoustic properties of crystals vary with their growth conditions [4]–[6]. Furthermore, James recently measured the acoustical physical constants of synthetic quartz [6], but he used the piezoelectric values published earlier by other investigators [7]. Because of this lack of precise knowledge, it is doubtful that the acoustic properties of quartz crystal substrates for SAW devices can be employed with a sufficiently high accuracy using the values of the constants published earlier, and this affects the present scientific and industrial world in which high performance quartz devices are required.

We have made highly precise measurements of the acoustic properties of various solids using bulk ultrasonic spectroscopy technology and have evaluated the acoustic properties and determined the elastic constants [8]–[12]. Recently, we have successfully determined all of the independent components of the acoustical physical constants of commercial $LiNbO_3$ and $LiTaO_3$ single crystals for SAW devices, providing the bulk wave velocities to four significant figures [13]. Quartz was used and studied long before $LiNbO_3$ and $LiTaO_3$ single crystals came into practical use, and many investigations were conducted regarding its acoustical physical constants. However, motivated by the uncertainties mentioned previously, in our recent preliminary study on the accuracy of the acoustical physical constants of quartz, we measured the longitudinal velocities of three principal X-, Y-, and Z-cut specimens and compared them with the values calculated from the constants reported in the papers most often cited and referenced [1]–[3], [6], [14]. We found differences exceeding 30 m/s (0.5%) in the Z-axis longitudinal velocity between the measured value and the calculated ones using the constants reported by Mason [1] and Bechmann *et al.* [2], which supported the need for precise measurements of the acoustical physical constants of synthetic quartz. By applying our technology to this problem, we believe that more accurate acoustical physical constants will be obtained, resulting in significantly useful benefits to high performance devices in the future.

In this paper, accurate values of the acoustical physical constants of synthetic quartz, commercially available and widely used for SAW devices, are determined. The optimal propagation directions and modes of bulk waves to obtain the most accurate constants possible are selected through numerical calculation. Three principal X-, Y-, and Z-cut specimens and several rotated Y-cut specimens (rotating a Y-cut specimen about the X axis) are prepared from a single crystal ingot to determine the constants and to confirm their accuracy. By measuring the longitudinal velocities, shear velocities, dielectric constants, and density

Manuscript received February 26, 2001; accepted July 16, 2001. This work was supported in part by the Research Grant-in-Aid from the Ministry of Education, Science and Culture of Japan, the Japan Society for the Promotion of Science for the Research for the Future Program.

The authors are with the Department of Electrical Engineering, Tohoku University, Sendai 980-8579, Japan (e-mail: kushi@ecei.tohoku.ac.jp).

with high accuracy, all of the independent components of the acoustical physical constants are determined.

II. Theoretical Consideration

The acoustical physical constants are determined from the velocities measured by the RF tone-burst pulse measurement method [15]. First, the Christoffel equations, relating velocities to the acoustical physical constants, are reviewed for a better understanding of the relationships among them. Proper propagation directions and modes are then selected by calculating the dependences of each constant on the bulk wave velocities to be measured.

A. Relationships Between Bulk Wave Velocities and the Constants

Quartz belongs to class 32 of the trigonal system in which there is a total of 11 independent acoustical physical constants. Taking the strain S and the electric field E as the independent variables, there are six elastic stiffness constants at constant electric field [c_{11}^E $(=c_{12}^E + 2c_{66}^E)$, c_{12}^E, c_{13}^E, c_{14}^E, c_{33}^E, and c_{44}^E], two piezoelectric stress constants (e_{11} and e_{14}), two dielectric constants at constant strain (ε_{11}^S and ε_{33}^S), and density (ρ). In this paper, the same determination procedure as used in the previous work [13] applies to determining the constants by measuring bulk wave velocities V that are related in the following general equation:

$$V = \sqrt{\frac{c^E + \frac{e^2}{\varepsilon^S}}{\rho}}. \tag{1}$$

From this equation, it can be understood that eight velocities, two dielectric constants, and density have to be measured in order to determine all of the acoustical physical constants. The dielectric constant ε_{11}^S can be measured using either X- or Y-cut specimen and ε_{33}^S can be measured using a Z-cut specimen.

It is desirable to use equations expressed in simpler forms. Therefore, we first investigate the relationships between constants and velocities for bulk acoustic waves propagating along the principal X, Y, and Z axes, and then choose several longitudinal waves and shear waves with independent particle displacement.

The X-axis longitudinal velocity $V_{X\ell}$ is related to the constants by

$$\rho V_{X\ell}^2 = c_{11}^E + \frac{e_{11}^2}{\varepsilon_{11}^S}, \tag{2}$$

and the Y-axis longitudinal velocity $V_{Y\ell}$ and Y-axis shear velocity with X-axis polarized particle displacement, V_{YsX}, are related to the constants by

$$\left(c_{11}^E - \rho V_{Y\ell}^2\right)\left(c_{44}^E - \rho V_{Y\ell}^2\right) - c_{14}^{E^2} = 0 \tag{3}$$

and

$$\rho V_{YsX}^2 = c_{66}^E + \frac{e_{11}^2}{\varepsilon_{11}^S}. \tag{4}$$

The Z-axis longitudinal velocity $V_{Z\ell}$ and degenerate shear velocity V_{Zs} are expressed as

$$\rho V_{Z\ell}^2 = c_{33}^E \tag{5}$$

and

$$\rho V_{Zs}^2 = c_{44}^E, \text{ respectively.} \tag{6}$$

The velocities of bulk waves propagating in the YZ plane are related to the acoustical physical constants in a simpler equation as well. The longitudinal velocity of bulk waves propagating in the YZ plane or along the thickness direction of a rotated Y-cut plate, $V_{rY\ell}$, and the shear velocity with X-axis polarized particle displacement, V_{rYsX}, are related to the constants by

$$\left(c_{11}^{E'} - \rho V_{rY\ell}^2\right)\left(c_{66}^{E'} - \rho V_{rY\ell}^2\right) - c_{16}^{E'^2} = 0 \tag{7}$$

and

$$\rho V_{rYsX}^2 = c_{55}^{E'} + \frac{e_{15}'^2}{\varepsilon_{11}^{S'}}. \tag{8}$$

The primed quantities indicate that the constants have been subjected to coordinate transformation for the desired propagation direction, and these constants are a function of the rotation angle θ for the rotated Y-cut specimen. The constants $c_{11}^{E'}$, $c_{66}^{E'}$, and $c_{16}^{E'}$ in (7) are all functions of the five elastic constants other than c_{12}^E:

$$\begin{aligned}
c_{11}^{E'} &= c_{11}^E \cos^4\theta + \frac{1}{2}c_{13}^E \sin^2 2\theta - 4c_{14}^E \cos^3\theta \cdot \sin\theta \\
&\quad + c_{33}^E \sin^4\theta + c_{44}^E \sin^2 2\theta, \\
c_{66}^{E'} &= \frac{1}{4}c_{11}^E \sin^2 2\theta - \frac{1}{2}c_{13}^E \sin^2 2\theta + \frac{1}{2}c_{14}^E \sin 4\theta \\
&\quad + \frac{1}{4}c_{33}^E \sin^2 2\theta + c_{44}^E \cos^2 2\theta, \text{ and} \\
c_{16}^{E'} &= -c_{11}^E \cos^3\theta \cdot \sin\theta + \frac{1}{4}c_{13}^E \sin 4\theta - c_{14}^E \cos\theta \cdot \cos 3\theta \\
&\quad + c_{33}^E \sin^3\theta \cdot \cos\theta + \frac{1}{2}c_{44}^E \sin 4\theta.
\end{aligned} \tag{9}$$

The constants $c_{55}^{E'}$, e_{15}', and $\varepsilon_{11}^{S'}$ in (8) are described in the following equations:

$$\begin{aligned}
c_{55}^{E'} &= c_{14}^E \sin 2\theta + c_{44}^E \sin^2\theta + c_{66}^E \cos^2\theta, \\
e_{15}' &= -e_{11}\cos^2\theta - \frac{1}{2}e_{14}\sin 2\theta, \text{ and} \\
\varepsilon_{11}^{S'} &= \varepsilon_{11}^S \cos^2\theta + \varepsilon_{33}^S \sin^2\theta.
\end{aligned} \tag{10}$$

By measuring $V_{Z\ell}$, V_{Zs}, and ρ, c_{33}^E and c_{44}^E can be obtained from (5) and (6), respectively. Also, three elastic constants, c_{11}^E, c_{13}^E, and c_{14}^E, can be determined with the

previously determined constants and three longitudinal velocities of three rotated Y-cut specimens including the Y-cut specimen, using (3) and (7), in which only the elastic constants and density are involved. By eliminating the term $e_{11}^2/\varepsilon_{11}^S$ from both (2) and (4), the following equation can then be obtained:

$$\rho\left(V_{X\ell}^2 - V_{YsX}^2\right) = c_{11}^E - c_{66}^E = \frac{c_{11}^E + c_{12}^E}{2}. \tag{11}$$

From (11), the elastic constant c_{12}^E $\left(=c_{11}^E - 2\,c_{66}^E\right)$ can be determined from measurements of $V_{X\ell}$ and V_{YsX}. It is seen that, following the procedure described so far, all of the elastic constants can be determined independently of the piezoelectric and dielectric constants.

The piezoelectric constant e_{11} can be obtained from (2) using the measured value of $V_{X\ell}$ and the previously determined c_{11}^E and measured ε_{11}^S. The piezoelectric constant e_{14} can be obtained from (8) using the shear velocity with X-axis polarized particle displacement for a rotated Y-cut specimen, V_{rYsX}, the previously determined constants, and the measured value of ε_{33}^S.

B. Selection of Rotated Y-Cut Specimens

Specimen plates, which determine the propagation directions of bulk waves, must be selected appropriately to determine the constants accurately. The rotated Y-cut specimens used in the measurements to determine the constants of c_{11}^E, c_{13}^E, c_{14}^E, and e_{14} were selected from the crystalline planes specified in the American Society for Testing and Materials (ASTM) Cards (No. 46-1045). Therefore, the inclination between the crystalline plane and the specimen surface can be measured by X-ray analysis, and the propagation directions or velocities of bulk waves are corrected by numerical methods.

In determining the constants of c_{11}^E, c_{13}^E, and c_{14}^E, or e_{14}, an appropriate combination of propagation directions must be selected considering the dependences of each constant and propagation direction on the bulk wave velocities. In this study, the propagation directions were selected to minimize the determination errors of the constants through numerical calculations following the subsequent procedure.

When the independent variables of the acoustical physical constants are denoted by x_i (i = 1 to 11), and the measured values of the velocities, dielectric constants, and density are denoted by y_j (j = 1 to 11), each measured value can be expressed as

$$y_j = f_j\left(x_1, x_2, \ldots, x_{11}\right). \tag{12}$$

When the measurement error Δy_j is contained in the measured value and the error in the constant to be determined is denoted by Δx_i, (12) can be expressed as

$$y_j + \Delta y_j = f_j\left(x_1 + \Delta x_1, x_2 + \Delta x_2, \ldots, x_{11} + \Delta x_{11}\right). \tag{13}$$

When (13) is expanded around variables x_i by Taylor's theorem and the second and higher order terms are ignored because of their minor errors, the equation for the errors is

$$\Delta y_j = \frac{\partial f_j}{\partial x_1}\Delta x_1 + \frac{\partial f_j}{\partial x_2}\Delta x_2 + \cdots + \frac{\partial f_j}{\partial x_{11}}\Delta x_{11}. \tag{14}$$

Solving (14) as simultaneous equations of j = 1 to 11, the following equation is then obtained:

$$\Delta x_i = a_{i1}\Delta y_1 + a_{i2}\Delta y_2 + \cdots + a_{i11}\Delta y_{11} \tag{15}$$

where a_{ij} is the (i,j)-component of the inverse matrix $[a]$ of the coefficient matrix $[\partial f/\partial x]$ in the simultaneous equations of (14) and varies with the combination of the propagation directions and modes of bulk waves used to determine the constants.

Because each measurement is carried out independently, the error in the constant is given by the square root of the sum of the squared terms,

$$\Delta x_i = \sqrt{\left(a_{i1}\Delta y_1\right)^2 + \left(a_{i2}\Delta y_2\right)^2 + \cdots + \left(a_{i11}\Delta y_{11}\right)^2}. \tag{16}$$

Because the matrix $[a]$ can be obtained numerically, selection of the combination of propagation directions that gives a small absolute value of the component a_{ij} leads to more accurate determination of the constants.

The longitudinal velocity changes for rotated Y-cut specimens were calculated when each of the elastic constants of c_{11}^E, c_{13}^E, and c_{14}^E varied within the range of $\pm 1\%$, using the values published in the literature [3]. The results are shown in Fig. 1. The velocity changes are represented as the coefficient $\partial f_j/\partial x_i$ in each term in (14). The matrix $[a]$ is calculated using the obtained velocity changes, and the combination of propagation directions, which produces the minimal error given by (16), is selected. The combination of the propagation directions [400] (Y-axis propagation), [021] (21.49°Y-axis propagation), and [304] (133.61°Y-axis propagation), shown by circles in Fig. 1, is chosen to determine the constants c_{11}^E, c_{13}^E, and c_{14}^E. To determine the constant e_{14}, a similar calculation is made, and the shear waves with X-axis polarized particle displacement in the [302] propagation direction (152.31°Y-axis propagation), in which the dependence of e_{14} on the velocity is the largest, was selected.

III. Experiments

A. Specimen Preparation

The quartz crystal ingot used in the measurements was a SAW-grade right-handed crystal for 3-in ST-cut wafers grown in an autoclave by Toyo Communication Equipment Co. The crystal growth conditions are shown in Table I. The seed crystal substrate was a Z-cut plate with dimensions of 80 mm (X) × 220 mm (Y) × 1.8 mm (Z), and the grown crystal dimensions were about 120 mm

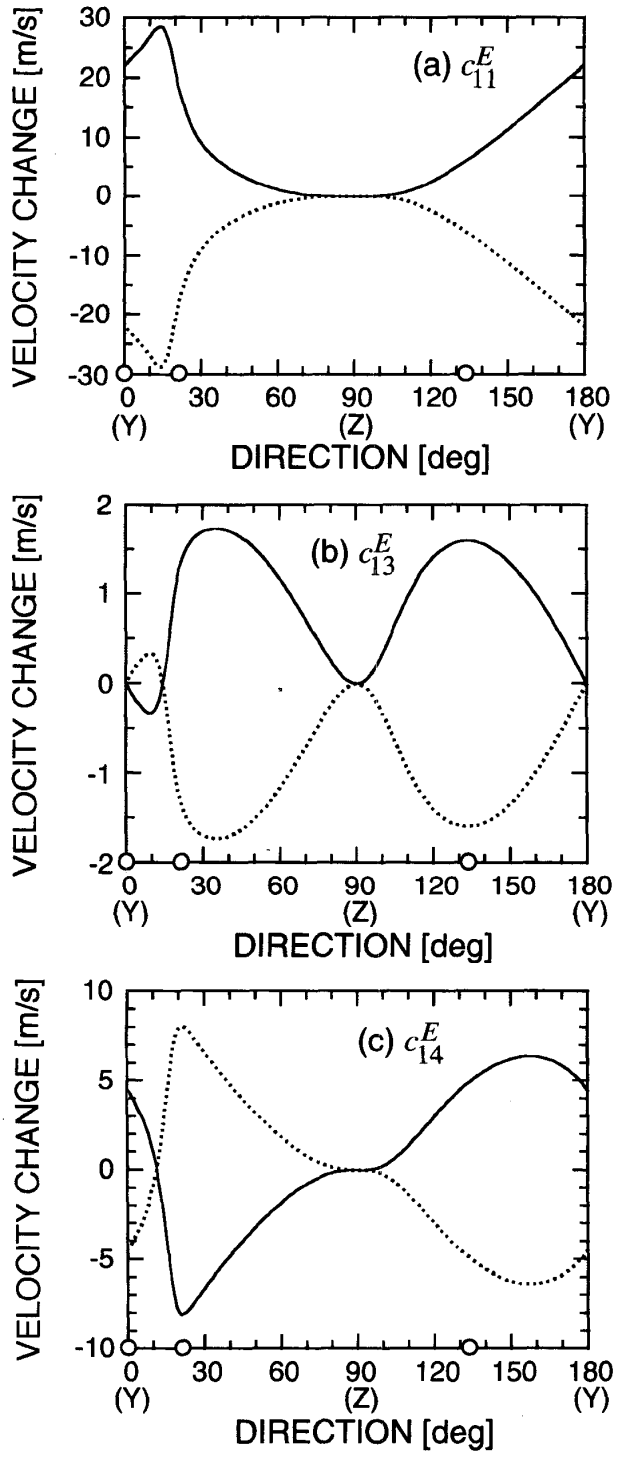

Fig. 1. Longitudinal velocity changes for rotated Y-cut specimen influenced by a 1% increase and decrease of the elastic constants of α-quartz. Solid line = +1%; dotted line = −1%.

TABLE I
CRYSTAL GROWTH CONDITIONS OF SYNTHETIC QUARTZ FOR SAW DEVICES.

Growth temperature	327°C
Temperature difference	44°C
Pressure	1160 kgf/cm^2
Run days	150 d
Growth rate	0.56 mm/d along Z axis
	0.25 mm/d along X axis

TABLE II
SPECIMENS USED FOR VELOCITY MEASUREMENTS.

	Plane	Prop. direction
Principal plane	(330)	X
	(400)	Y
	(006)	Z
Crystalline plane	(021)	21.49° Y
	(033)	38.21° Y
	(023)	49.74° Y
	(015)	75.75° Y
	(304)	133.61° Y
	(303)	141.79° Y
	(302)	152.31° Y
Device plane	BT	49.13° Y
	LST	75° Y
	ST	137.25° Y
	AT	144.78° Y

$(X) \times 220$ mm $(Y) \times 80$ mm (Z). The ingot was lumbered into 75 mm $(X) \times 160$ mm $(Y) \times 75$ mm (Z) and was then divided into two pieces of Z-cut plates with the seed crystal plate removed and dimensions of 75 mm $(X) \times 160$ mm $(Y) \times 32$ mm (Z). The quality of synthetic quartz differs from one growth zone to another because of variations in growth rate: only the portion grown in the direction of the Z axis on the seed plate, called the Z-axis growth zone, is of the highest quality and sufficient for devices [16]. All of the specimens used in the measurements were prepared from the Z-axis growth zone. The specimens used to measure bulk wave velocities, dielectric constants, and density were taken from the same ingot.

Table II shows the specimens prepared for velocity measurements. We prepared six specimens for velocity measurements to determine the constants, selected in accordance with the previous, theoretical consideration, as well as other specimens to confirm the accuracy of the determined constants, including four specimens practically used for devices such as AT-cut and BT-cut substrates for the thickness-shear mode, and ST-cut and LST-cut substrates for SAWs, which exhibit excellent frequency-temperature characteristics. All of the specimens for velocity measurements were about 4 mm thick, and both major faces were optically polished. The flatness around the center, where velocity measurements are conducted, was within $\lambda/10$ ($\lambda = 0.633$ μm), and the deviation from parallelism was less than 9's.

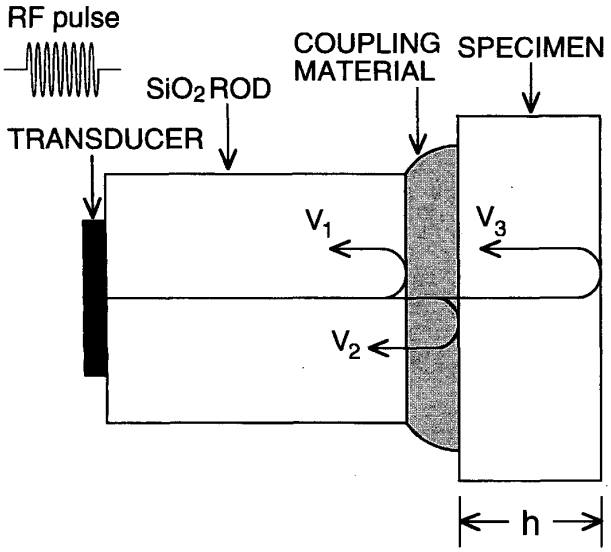

Fig. 2. Experimental arrangement of bulk wave ultrasonic velocity measurements of solid specimens using bulk ultrasonic RF pulses.

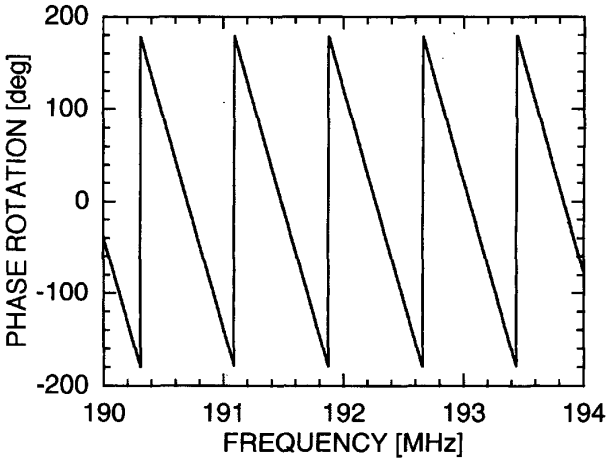

Fig. 3. An example of frequency response of phase rotation measured for Z-axis longitudinal velocity.

In the measurements made by the RF pulse measurement method in this study, the propagation direction of the ultrasonic waves was perpendicular to the specimen surface. Because the velocity is a function of the propagation direction, the propagation direction must be known to high accuracy for the highly accurate determination of the acoustical physical constants of this study. It is seen that the ratio of the lattice constant a to the lattice constant c is needed to obtain the rotation angle of the rotated Y-cut specimens. Therefore, the lattice constants a and c were measured with the Cu$K\alpha_1$ line by an X-ray diffractometer using the Bond method [17]. Furthermore, the inclination angle of the specimen surface from the crystalline plane was also checked. The inclination angles were very small, viz., 0.014° maximum, and were used to correct the velocity values.

B. Measurement Method

Velocity measurements were made by the complex-mode measurement method [15] using RF tone burst pulse signals. The experimental arrangement is shown in Fig. 2. The ultrasonic device consists of a transducer fabricated on one end of a synthetic silica (SiO_2) glass buffer rod, which transmits RF pulse signals to the specimen via the couplant. A ZnO piezoelectric thin-film transducer and an X-cut $LiNbO_3$ plate transducer were used to generate the longitudinal waves and shear waves, respectively.

For longitudinal wave measurements, pure water is used as the coupling material with an appropriate setting of the distance between the ultrasonic device and the specimen, so the reflected signal from the front surface of the specimen, V_2, can be separated from the reflected signal from the SiO_2 buffer rod end, V_1, in the time domain. The phases of the reflected signals from the front surface, V_2, and from the back surface, V_3, are measured, and by subtracting the phase of V_2 from the phase of V_3, the sum of the phase rotation in the specimen, $-2kh$, and the phase rotation at the perfect reflection on the back surface of the specimen, π,

$$\phi = -2kh + \pi, \tag{17}$$

is extracted. The phase rotation ϕ measured for the longitudinal wave propagation for the Z-cut specimen is given in Fig. 3. In (17), k and h are the wave number in the specimen and the thickness of the specimen, respectively, and k is related to the velocity in the specimen, V, and the angular frequency, ω, as $k = \omega/V$. Thus, by measuring ϕ and h, we can obtain V as follows:

$$V = -\frac{2\omega h}{\phi - \pi}. \tag{18}$$

For shear wave measurements, salol (phenyl salicylate) is used as the coupling material with a typical thickness of $< 1\mu$m to bond the specimen to the buffer rod end, so the reflected signal from the front surface, V_2, cannot be separated from the reflected signal from the rod end, V_1, in the time domain. As a result, the phase rotation ΔTR at the transmission or reflection at the bonding layer is contained in the phase rotation ϕ to be measured. The phase rotation ΔTR at the bonding layer can be calculated with knowledge of the acoustic parameters (velocity, attenuation coefficients, and density) of the bonding layer and by estimating the layer thickness by comparing measured and calculated frequency dependences of the reflection coefficient at the boundary between the SiO_2 buffer rod and the bonding layer. Thus, the shear wave velocity is given by

$$V = -\frac{2\omega h}{\phi - \pi - \Delta TR}. \tag{19}$$

The thicknesses of the specimens were measured with a digital length gauging system (CERTO; Dr. Johannes

Heidenhain GmbH, Traunreut, Germany) with an optical encoder.

The dielectric constants are obtained from the capacitance measurement for a plate with full electrodes of thin Al films evaporated on both surfaces [18]. The capacitance at a lower frequency, C^T, is given by

$$C^T = \varepsilon^T \frac{S}{h}, \tag{20}$$

where ε^T, S, and h are the dielectric constants at constant stress, the electrode area, and the thickness of the specimen, respectively. The plate capacitance can be measured with an impedance analyzer (Model HP4294A; Hewlett-Packard Co.). The electrode area of the plate can be obtained from the volume of the plate, calculated from the measured plate weight in air and the densities of air and the plate, and the measured plate thickness [19]. The dielectric constant at constant strain, ε_{ij}^S, is then obtained from ε_{ij}^T using the following equation:

$$\varepsilon_{ij}^S = \varepsilon_{ij}^T - e_{ip} s_{pq}^E e_{qj} \tag{21}$$

where s^E is the elastic compliance constant at constant electric field and is related to the elastic stiffness constant c^E as $s^E = (c^E)^{-1}$. For quartz, ε_{11}^S and ε_{11}^T are not equal, but ε_{33}^S is equal to ε_{33}^T.

The density is determined by the Archimedes method by weighing the specimen both in air and in water [20].

C. Results

The measured specimen thicknesses and bulk velocities used for determination are given in Table III. The measurement errors in velocity are given by the maximum deviation of the phase rotation in the measurement frequency range and the measurement accuracy of the specimen thickness. To reduce the influence of the diffraction effect on the velocity measurements, a higher frequency range was chosen, viz., 165 to 220 MHz for longitudinal waves and 115 to 150 MHz for shear waves. The entire measurement system was operated in a temperature-controlled room, where the room temperature was maintained at 23 ± 0.1°C, and the specimen, couplant, and ultrasonic device were placed in a chamber whose temperature was controlled to within ±0.01°C. During the phase rotation measurements, the temperatures of the water couplant for longitudinal waves and of the air around the specimen for shear waves were monitored with a copper-constantan thermocouple (JIS T-Model, Class 1; CHINO Co.). The thermocouple was calibrated to within ±0.01°C by a platinum resistance thermometer (Model R800-2; CHINO Co.). All specimens were measured at 23.0 ± 0.1°C, and the temperature deviation during all of the measurements was within ±0.01°C. For all of the specimens used to determine the constants, velocities were also measured at 20°C and 26°C. Corrected velocity values at 23.00°C were obtained using the measured temperature dependences of velocities that were determined with measured phase rotations and specimen thicknesses calculated from the measured thicknesses at 23°C and thermal expansion coefficients reported in the literature [3]. The correction values are very small: 0.05 m/s, maximum. The thickness variation for a 4-mm-thick specimen caused by the temperature variation of 6°C is very small: about 0.3 μm, maximum. This allows the specimen thicknesses at each temperature to be obtained with sufficient accuracy from the calculation using the published thermal expansion coefficients. Fig. 4 shows the temperature dependences of the velocities of longitudinal and shear waves propagating along the Z axis. The straight lines in the figure are the least squares approximated lines for three measured values. Similar linear temperature dependences were observed for other specimens. The deviations of measured velocities from the approximated lines for either longitudinal or shear waves are very small: 0.016 m/s, maximum. The deviation from parallelism of all of the specimens used in the measurements was less than 9's. The influence of the parallelism is negligible in the measurements of phase rotation, i.e., < 0.1 ppm.

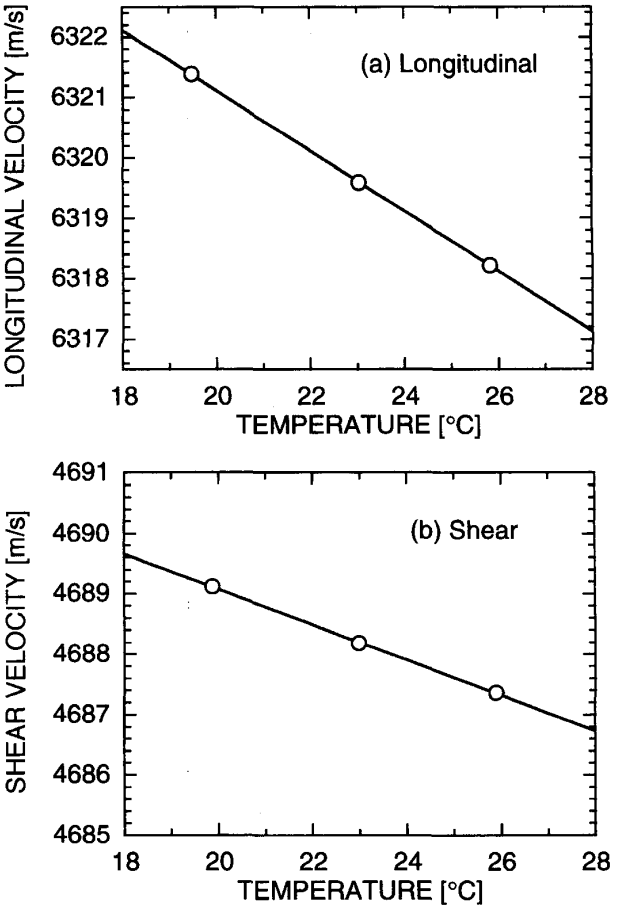

Fig. 4. Temperature dependences of Z-axis longitudinal and shear velocities.

TABLE III
MEASURED RESULTS OF SPECIMEN THICKNESSES AND BULK WAVE VELOCITIES USED FOR DETERMINATION.

Mode	Specimen		Thickness (μm)	Velocity (m/s)
Longitudinal wave	(330)	X	4034.96 ± 0.10	5749.46 ± 0.25
	(400)	Y	4035.79 ± 0.10	6005.94 ± 0.20
	(006)	Z	4034.71 ± 0.10	6319.62 ± 0.30
	(021)	21.49° Y	4029.36 ± 0.10	5372.08 ± 0.28
	(304)	133.61° Y	4029.38 ± 0.10	7012.94 ± 0.26
Shear wave	(400)	Y	4035.79 ± 0.10	3916.95 ± 0.16
	(006)	Z	4034.71 ± 0.10	4688.50 ± 0.14
	(302)	152.31° Y	4029.49 ± 0.10	3327.98 ± 0.13

TABLE IV
MEASURED DIELECTRIC CONSTANTS.

$\varepsilon_{11}^T/\varepsilon_0$	4.507 ± 0.011
$\varepsilon_{11}^S/\varepsilon_0$	4.420 ± 0.011
$\varepsilon_{33}^T/\varepsilon_0$, $\varepsilon_{33}^S/\varepsilon_0$	4.628 ± 0.011

TABLE V
MEASURED DENSITIES.

Specimen	Density (kg/m^3)
Y-cut	2648.66 ± 0.05
Z-cut	2648.68 ± 0.05
Average	2648.67 ± 0.05

The digital length gauging system, placed on a vibration isolation system to remove any small vibrations occurring in the measurement environment, is capable of measuring specimen thickness with a reproducibility of ±0.02 μm. The gauging system was also operated in a temperature-controlled chamber to realize stable measurements, taking into consideration the influence of the linear thermal expansion coefficients of the specimens. We can guarantee an absolute accuracy of ±0.10 μm through comparative measurement using several standard guage blocks (Class K; Mitutoyo Co.)

The dielectric constants of ε_{11}^T and ε_{33}^T were measured with the X-cut and Z-cut specimens, respectively. The thickness of each specimen was chosen to be 0.5 mm to reduce the influence of edge capacitance; the larger electrode areas of the specimens were used to account for the measurement accuracy of the impedance analyzer: about 60 mm (Y) × 32 mm (Z) for the X-cut specimen and about 75 mm (X) × 40 mm (Y) for the Z-cut specimen. The measured capacitance was corrected for the effect of edge capacitance using a well-accepted method [21]. The obtained values of the dielectric constants are given in Table IV. The measurements were made around 10 kHz in the temperature-controlled room maintained at 23.0 ± 0.1°C. Consequently, the results were scarcely affected by temperature variation. The measurement errors are given by the accuracy of the measurement instruments used and the variations in the values obtained from the multiple measurements carried out.

Densities were measured for the two Y- and Z-cut specimens prepared from two different parts of the crystal ingot. The results are given in Table V. The measurement errors are given by considering the variations in the measured weight values obtained from the multiple measurements conducted and also those in the measured values for temperature, pressure, and humidity that are needed to obtain the densities of air [22] and water [23] in the literature. No significant difference larger than the measurement error was observed for the two specimens. The influence of a measurement temperature variation of $< \pm 0.02$°C is less than the measurement error because the density measurement system was also placed in the temperature-controlled room (23.0 ± 0.1°C).

IV. DISCUSSION

The determined acoustical physical constants of synthetic quartz are given in Table VI together with those of four previous reports [1]–[3], [6]. The errors in the determined constants were calculated using (16). Because the previously published values were not obtained at 23°C, calculation was made to obtain the values at that temperature using the temperature coefficients in the respective literature reports.

To confirm the accuracy of the determined constants, the measured velocity values of bulk acoustic waves that were not used for the determination were compared with those calculated from the determined constants. The results for longitudinal velocities and shear velocities with X-axis polarized particle displacement are given in Table VII and VIII, respectively. The differences between the measured and calculated longitudinal velocities are <0.15 m/s. The differences in shear velocity with X-axis polarized particle displacement are < 0.20 m/s, although data for only two specimens are available for the comparison. The shear wave velocities with X-axis polarized particle displacement measured for the AT- and BT-cut specimens are related to the thickness-shear mode used for bulk acoustic wave devices. From these results, we deduce that the determined constants are highly accurate, yielding bulk acoustic wave velocities with an accuracy of ±0.004%.

TABLE VI

MEASURED AND PREVIOUSLY PUBLISHED ACOUSTICAL PHYSICAL CONSTANTS OF SYNTHETIC QUARTZ.

		Measured	Mason [1]	Bechmann *et al.* [2]	Koga *et al.* [3]	James [6]
Elastic constant ($\times 10^9$ N/m^2)	c_{11}^E	86.7997 ± 0.0079	86.06	86.73	86.820 ± 0.015	86.798 ± 0.013
	c_{12}^E	7.0362 ± 0.0183	5.08	6.93	7.036 ± 0.051	6.8260 ± 0.037
	c_{13}^E	11.9376 ± 0.0190	10.46	11.89	11.917 ± 0.028	12.023 ± 0.18
	c_{14}^E	18.0612 ± 0.0046	18.25	17.92	18.0695 ± 0.0038	18.112 ± 0.063
	c_{33}^E	105.7816 ± 0.0103	107.1	107.1	105.88 ± 0.12	105.827 ± 0.021
	c_{44}^E	58.2231 ± 0.0037	58.67	57.91	58.2267 ± 0.0065	58.232 ± 0.018
	c_{66}^E	39.8817 ± 0.0131	40.49	39.90	39.892 ± 0.018	39.986 ± 0.017
Piezoelectric constant (C/m^2)	e_{11}	0.1719 ± 0.0013	0.167	0.171	0.175	0.1712 ± 0.00094
	e_{14}	0.0390 ± 0.0025	0.0324	0.0403	0.0407	0.0407
Dielectric constant	$\varepsilon_{11}^S/\varepsilon_0$	4.420 ± 0.011	4.50	4.428	4.50	4.423
	$\varepsilon_{33}^S/\varepsilon_0$	4.628 ± 0.011	4.70	4.634	4.50	4.635 ± 0.011
Density ($\times 10^3$ kg/m^3)	ρ	2.64867 ± 0.00005	2.654	2.65	2.6484	2.64857 ± 0.00003

TABLE VII

COMPARISON OF LONGITUDINAL VELOCITIES MEASURED FOR OTHER QUARTZ SPECIMENS WITH THOSE CALCULATED FROM THE DETERMINED CONSTANTS.

Specimen		Measured (m/s)	Calculated (m/s)	Difference (m/s)
(033)	38.21° Y	5894.59	5894.47	−0.12
(023)	49.74° Y	6174.41	6174.42	+0.01
(015)	75.75° Y	6364.12	6364.11	−0.01
(303)	141.79° Y	7031.67	7031.71	+0.04
(302)	152.31° Y	6927.06	6927.05	−0.01
AT	144.78° Y	7016.89	7016.97	+0.08
BT	49.13° Y	6162.62	6162.56	−0.06
ST	137.25° Y	7031.86	7031.81	−0.05
LST	75° Y	6366.01	6365.97	−0.04

TABLE VIII

COMPARISON OF SHEAR VELOCITIES WITH X-AXIS POLARIZED PARTICLE DISPLACEMENT MEASURED FOR OTHER QUARTZ SPECIMENS WITH THOSE CALCULATED FROM THE DETERMINED CONSTANTS.

Specimen		Measured (m/s)	Calculated (m/s)	Difference (m/s)
AT	144.78° Y	3320.08	3320.16	+0.08
BT	49.13° Y	5084.15	5083.97	−0.18

TABLE IX
MEASURED LONGITUDINAL VELOCITIES AND THE DIFFERENCES BETWEEN THE MEASURED AND CALCULATED FROM THE PUBLISHED CONSTANTS.

Specimen		Measured (m/s)	Difference (m/s) Mason [1]	Bechmann *et al.* [2]	Koga *et al.* [3]	James [6]
(330)	X	5749.46	−31.91	−4.05	+1.39	−0.18
(400)	Y	6005.94	−17.32	−8.61	+1.05	+1.37
(006)	Z	6319.62	+32.87	+37.66	+3.26	+1.48
(021)	21.49° Y	5372.08	−32.28	−2.60	+0.32	−0.95
(304)	133.61° Y	7012.94	−6.14	−6.50	+1.18	+3.18
(033)	38.21° Y	5894.59	−11.68	+2.35	+0.71	+0.45
(023)	49.74° Y	6174.41	−0.54	+9.78	+1.41	+1.16
(015)	75.75° Y	6364.12	+25.06	+30.25	+2.79	+1.56
(303)	141.79° Y	7031.67	−10.20	−10.00	+1.10	+3.29
(302)	152.31° Y	6927.06	−13.85	−12.34	+0.97	+3.07
AT	144.78° Y	7016.89	−11.37	−10.85	+1.11	+3.30
BT	49.13° Y	6162.62	−1.21	+9.28	+1.31	+1.07
ST	137.25° Y	7031.86	−8.18	−8.34	+1.07	+3.18
LST	75° Y	6366.01	+24.37	+29.64	+2.73	+1.54

TABLE X
MEASURED SHEAR VELOCITIES WITH X-AXIS POLARIZED PARTICLE DISPLACEMENT AND THE DIFFERENCES BETWEEN MEASURED AND CALCULATED FROM THE PUBLISHED CONSTANTS.

Specimen		Measured (m/s)	Difference (m/s) Mason [1]	Bechmann *et al.* [2]	Koga *et al.* [3]	James [6]
(400)	Y	3916.95	+22.60	−0.57	+1.33	+4.76
(006)	Z	4688.50	+13.23	−13.80	+0.38	+0.45
(302)	152.31° Y	3327.98	+19.54	+2.27	+0.71	+1.99
AT	144.78° Y	3320.08	+17.80	+1.22	+0.58	+1.18
BT	49.13° Y	5084.15	+19.71	−12.99	+1.07	+3.71

Next, the measured velocity values were compared with those calculated from the constants published in the literature [1]–[3], [6]. The results obtained for longitudinal velocity and shear velocity with X-axis polarized particle displacement are given in Table IX and X, respectively. Mason's constants provided the largest average difference between our measured and calculated values, followed by those of Bechmann *et al.*, James, and Koga *et al.*, in that order, both for the longitudinal and shear waves. Even for the constants of Koga *et al.*, the calculated velocity values, which were closest to our measured values, differ > 3 m/s for the worst propagation directions of longitudinal waves. The constants of Mason, Bechmann *et al.*, and Koga *et al.* gave the largest differences between the measured and calculated values in Z-axis longitudinal velocity. It is considered that, from (5), this is related to the accuracy of c_{33}^E. It is seen from Table VI that the values of c_{33}^E of Mason and Bechmann *et al.* differ significantly from the determined values, although that of Koga *et al.* differs slightly. It may be interesting to note that all of these three constants were determined using the resonance method. In the resonance method, because the Z-axis longitudinal velocity, uncoupled with piezoelectricity, cannot be measured directly, the elastic constant c_{33}^E is calculated using multiple simultaneous equations for piezoelectric vibrations with other specimens. That is speculated to lead to an inaccurate determination of the constant, resulting in the considerably large difference between the measured and calculated Z-axis longitudinal velocities. In contrast, our measured value of c_{33}^E is very accurate because of the determination using the simple form of (5), only with the Z-axis longitudinal velocity and density. It is, therefore, considered that James' values are relatively accurate because he measured the velocities using the pulse measurement method. The difference in Z-axis longitudinal velocity between the measured and calculated velocities is 1.48 m/s, which is the smallest difference among the four values calculated using the constants in the four respective references. This difference, however, is not small enough to ignore, compared with the current measurement accuracy of velocity. The velocities calculated with James' constants differ significantly from the measured values in other propagation directions as well; the average difference in longitudinal velocity is about 1.8 m/s, and that in shear velocity about 2.4 m/s.

The temperature coefficients of the elastic and piezo-

TABLE XI
MEASURED AND PREVIOUSLY PUBLISHED TEMPERATURE COEFFICIENTS OF THE ACOUSTICAL PHYSICAL CONSTANTS OF SYNTHETIC QUARTZ.

		Measured (23°C)	Mason (25°C) [1]	Bechmann *et al.* (25°C) [2]	Koga *et al.* (20°C) [3]	James (25°C) [6]
Elastic constant ($\times 10^{-6}$/°C)	$T_{c^E 11}$	−45.5	−46.5	−48.5	−44.4	−43.591
	$T_{c^E 12}$	−2440	−3300	−3000	−2563	−2640.1
	$T_{c^E 13}$	−745	−700	−550	−492	−592.27
	$T_{c^E 14}$	98.7	90	101	98.4	102.59
	$T_{c^E 33}$	−193	−205	−160	−188	−190.32
	$T_{c^E 44}$	−160	−166	−177	−172	−171.59
	$T_{c^E 66}$	166	164	178	180	176.79
Piezoelectric constant ($\times 10^{-4}$/°C)	T_{e11}	−0.67			−1.8	−1.6
	T_{e14}	−14.4			−2.4	−14.4
Dielectric constant ($\times 10^{-5}$/°C)	$T_{\varepsilon^S 11/\varepsilon 0}$					1.47
	$T_{\varepsilon^S 33/\varepsilon 0}$					1.88
Density ($\times 10^{-6}$/°C)	T_ρ	−34.96 [3]	−36.4	−34.92	−34.96	−35.02
Thermal expansion ($\times 10^{-6}$/°C)	α_{11}	13.74 [3]	14.3	13.71	13.74	13.77
	α_{33}	7.48 [3]	7.8	7.48	7.48	7.483

electric constants in the measured temperature range of 20 to 26°C are shown in Table XI compared with the published values [1]–[3], [6]. The temperature coefficients of the dielectric constants are very small, so the constants are assumed to be constant in the temperature range. The published values of the thermal expansion coefficients were employed to calculate the temperature coefficient of density. The variation of density caused by the temperature variation of 6°C is estimated to be < 0.6 kg/m^3. In the same way as for specimen thickness, densities at each temperature can be accurately estimated using the published values of the thermal expansion coefficients. The velocity variations for the temperature variation of 6°C are 0.04 to 3.0 m/s, depending on the propagation directions and modes, which are about 100 times greater than the differences of 0.0008 to 0.016 m/s between the measured velocities and approximated lines for the velocity-temperature dependences. Therefore, the significant figures in the temperature coefficient measurements are approximately three digits. Comparing the measured and published values, we can see the significant differences in c_{12}^E and c_{13}^E.

The major causes of these differences between the constants determined in our work and those published previously are considered to be different quartz quality (e.g., Mason's material was natural quartz), propagation directions, and methods used for the measurements.

V. SUMMARY

In this paper, we reported determination of all of the independent components of the acoustical physical constants of synthetic α-quartz crystal, commercially available and widely used for SAW devices. We considered carefully the most proper propagation directions and modes for accurately determining the constants of quartz through numerical calculations, and established the experimental procedures. Three principal X-, Y-, and Z-cut specimens and three rotated Y-cut specimens [(021), (304), and (302) crystalline planes] for accurately determining the constants were prepared from one SAW-grade synthetic quartz ingot, and eight additional, rotated Y-cut specimens, including AT-, BT-, ST-, and LST-cut substrates for devices, were prepared to confirm the determination accuracy. The longitudinal velocities, shear velocities, dielectric constants, and density were measured with high accuracy. The velocity values measured for the specimens that were not used for the determination agreed very well with the values calculated from the newly determined constants. The differences between the measured and calculated velocities of either longitudinal or shear waves were < 0.20 m/s. These results provide the constants that give bulk acoustic wave velocities with an accuracy of $\pm 0.004\%$.

ACKNOWLEDGMENTS

The authors are grateful to K. Nagai of Toyo Communication Equipment Co., Ltd. for supplying the crystals; Y. Okada of Kougakugiken Co., Ltd. for preparing the specimens; K. Fujii of the National Research Laboratory of Metrology for discussing accurate measurements of the density; M. Arakawa and R. Okabe for measuring the densities and specimen thicknesses; and J. Hirohashi for analyzing the specimen surface by an X-ray diffractometer using the Bond method.

REFERENCES

[1] W. P. Mason, "Properties and uses of quartz crystals," in *Piezoelectric Crystals and Their Application to Ultrasonics.* New York: D. Van Nostrand Co., 1950, pp. 78–113.

[2] R. Bechmann, A. D. Ballato, and T. J. Lukaszek, "High-order temperature coefficients of the elastic stiffnesses and compliances of alpha-quartz," *Proc. IRE*, vol. 50, pp. 1812–1822, Aug. 1962.

[3] I. Koga, M. Aruga, and Y. Yoshinaka, "Theory of plane elastic waves in a piezoelectric crystalline medium and determination of elastic and piezoelectric constants of quartz," *Phys. Rev.*, vol. 109, pp. 1467–1473, Mar. 1958.

[4] R. Bechmann, "Frequency-temperature-angle characteristics of AT-type resonators made of natural and synthetic quartz," *Proc. IRE*, vol. 44, pp. 1600–1607, Nov. 1956.

[5] S. N. Baranovskiĭ and V. I. Panov, "Effect of uniaxial compression on the piezoelectric modulus of quartz," *Sov. Phys. Acoust.*, vol. 20, pp. 71–72, Jul.–Aug. 1974.

[6] B. J. James, "A new measurement of the basic elastic and dielectric constants of quartz," in *Proc. 42nd Annu. Freq. Contr. Symp.*, pp. 146–154, 1988.

[7] R. K. Cook and P. G. Weissler, "Piezoelectric constants of alpha- and beta-quartz at various temperatures," *Phys. Rev.*, vol. 80, pp. 712–716, Nov. 1950.

[8] J. Kushibiki, T. Wakahara, T. Kobayashi, and N. Chubachi, "A calibration method of the LFB acoustic microscope system using isotropic standard specimens," in *Proc. 1992 IEEE Ultrason. Symp.*, pp. 719–722, 1992.

[9] J. Kushibiki and I. Takanaga, "Elastic properties of single- and multi-domain crystals of $LiTaO_3$," *J. Appl. Phys.*, vol. 81, pp. 6906–6910, May 1997.

[10] J. Kushibiki and M. Arakawa, "A method for calibrating the line-focus-beam acoustic microscopy system," *IEEE Trans. Ultrason., Ferroelect., Freq. Contr.*, vol. 45, pp. 421–430, Mar. 1998.

[11] I. Takanaga and J. Kushibiki, "Elastic constants of multidomain $LiTaO_3$ crystal," *J. Appl. Phys.*, vol. 86, pp. 3342–3346, Sep. 1999.

[12] J. Kushibiki, T.-C. Wei, Y. Ohashi, and A. Tada, "Ultrasonic microspectroscopy characterization of silica glass," *J. Appl. Phys.*, vol. 87, pp. 3113–3121, Mar. 2000.

[13] J. Kushibiki, I. Takanaga, M. Arakawa, and T. Sannomiya, "Accurate measurements of the acoustical physical constants of $LiNbO_3$ and $LiTaO_3$ single crystals," *IEEE Trans. Ultrason., Ferroelect., Freq. Contr.*, vol. 46, pp. 1315–1323, Sep. 1999.

[14] J. Kushibiki, S. Nishiyama, and I. Takanaga, "Measurements of bulk acoustic properties of synthetic α-quartz," *Electron. Lett.*, vol. 36, pp. 928–929, May 2000.

[15] J. Kushibiki and M. Arakawa, "Diffraction effects on bulk-wave ultrasonic velocity and attenuation measurements," *J. Acoust. Soc. Amer.*, vol. 108, pp. 564–573, Aug. 2000.

[16] J. Yoshimura, T. Miyazaki, T. Wada, K. Kohra, M. Hosaka, T. Ogawa, and S. Taki, "Measurement of local variations in spacing and orientation of lattice plane of synthetic quartz," *J. Cryst. Growth*, vol. 46, no. 5, pp. 691–700, 1979.

[17] W. L. Bond, "Precision lattice constant determination," *Acta Cryst.*, vol. 13, pp. 814–818, 1960.

[18] *IEEE Standard on Piezoelectricity*, IEEE Standard 176, 1987.

[19] *Standard Test Methods for A-C Loss Characteristics and Permittivity (Dielectric Constant) of Solid Electrical Insulating Materials*, ASTM Standard D150-81, 1981.

[20] H. A. Bowman and R. M. Schoonover, "Procedure for high precision density determinations by hydrostatic weighing," *J. Res. Nat. Bur. Stand.*, vol. 71C, pp. 179–198, Jul.–Aug. 1967.

[21] A. H. Scott and H. L. Curtis, "Edge correction in the determination of dielectric constant," *J. Res. Nat. Bur. Stand.*, vol. 22, pp. 747–775, Jun. 1939.

[22] R. S. Davis, "Equation for the determination of the density of moist air (1981/91)," *Metrologia*, vol. 29, no. 1, pp. 67–70, 1992.

[23] F. E. Jones and G. L. Harris, "ITS-90 density of water formulation for volumetric standards calibration," *J. Res. Nat. Inst. Stand. Tech.*, vol. 97, pp. 335–340, May–Jun. 1992.

Jun-ichi Kushibiki (M'83) was born in Hirosaki, Japan on November 23, 1947. He received the B.S., M.S., and Ph.D. degrees in electrical engineering from Tohoku University, Sendai, Japan, in 1971, 1973, and 1976, respectively.

In 1976, he became a research associate at the Research Institute of Electrical Communication, Tohoku University. In 1979, he joined the Department of Electrical Engineering, Faculty of Engineering, Tohoku University, where he was an associate professor from 1988 to 1993 and became a professor in 1994. He has been studying ultrasonic metrology, especially acoustic microscopy and its applications, and has established a method of material characterization by line-focus-beam acoustic microscopy. He also has been interested in biological tissue characterization in the higher frequency range, applying both bulk and acoustic microscopy techniques.

Dr. Kushibiki is a fellow of the Acoustical Society of America and a member of the Institute of Electronics, Information and Communication Engineers of Japan, the Institute of Electrical Engineers of Japan, the Acoustical Society of Japan, and the Japan Society of Ultrasonics in Medicine.

Izumi Takanaga (M'00) was born in Toyama Prefecture, Japan on February 3, 1973. She received the B.S., M.S., and Ph.D. degrees in electrical engineering from Tohoku University, Sendai, Japan, in 1995, 1997, and 2000, respectively.

Since 2000, she has been a research associate at the Department of Electrical Engineering, Faculty of Engineering, Tohoku University. Her research interests include accurate measurements of the elastic properties of piezoelectric materials and investigation of the domain structures of ferroelectric materials.

Dr. Takanaga is a member of the Acoustical Society of Japan.

Shouichi Nishiyama was born in Fukushima Prefecture, Japan on July 30, 1974. He received the B.S. and M.S. degrees in electrical engineering from Tohoku University, Sendai, Japan, in 1998 and 2000, respectively.

Since 2000, he has been working at Matsushita Electronic Components Co., Ltd., Osaka, Japan.